Astron. Astrophys. 115, 104–114 (1982)

ASTRONOMY AND ASTROPHYSICS

Empirical NLTE Analyses of Solar Spectral Lines

III. Iron Lines Versus LTE Models of the Photosphere

R. J. Rutten[1] and R. I. Kostik[2]

[1] Sterrewacht "Sonnenborgh" The Astronomical Institute, Zonnenburg 2, 3512 NL Utrecht, The Netherlands
[2] Main Astronomical Observatory, Ukrainian Academy of Sciences, SU-252127 Kiev-127, USSR

Received May 18, accepted July 12, 1982

Summary. We compare observational indications of departures from LTE in solar Fe I lines with published NLTE computations, in the context of discrepancies between empirical LTE and NLTE models of the solar atmosphere. We find that the importance of departures from LTE in Fe I and similar spectra is often underestimated through neglect of opacity departures. We demonstrate with numerical experiments that the peculiarities of the LTE models are artifacts due to the neglect of NLTE departures; in particular, we so explain the Holweger-Müller LTE model quantitatively. However, we show also that the NLTE formation of most optical metal lines is fortuitously well-mimicked by LTE computation when using LTE models. Thus, LTE-derived metal abundances and empirical oscillator strengths happen to be fairly precise. The same may hold for the use of theoretical radiative-equilibrium models in stellar abundance determinations.

Key words: stellar photospheres – solar abundances – empirical solar models – line formation – iron lines

I. Introduction

The Fe I spectrum is of particular interest in studies of solar-type photospheres because it represents the prime source of optical spectral-line diagnostics. In the solar spectrum Fe I is the only spectral species furnishing an appreciable number of unblended lines without isotope or hyperfine structure splitting: 402 in the list by Stenflo and Lindegren (1977) covering the current magnetic tape edition of the Jungfraujoch Atlas (Delbouille et al., 1973). The majority of the useful "magnetic" lines compiled by Harvey (1973) and of the "velocity" lines compiled by Sistla and Harvey (1970), respectively of high and zero Landé factor, are therefore due to Fe I.

In addition, Fe I is one of the few spectral species for which accurate laboratory data are available. Dravins et al. (1981) combine the laboratory wavelengths and levels of Crosswhite (1975) with the list of Stenflo and Lindegren into a list of 311 unblended solar lines with known wavelengths. The Oxford group contributes high-precision measurements of Fe I transition probabilities in steadily increasing number (Blackwell and Shallis, 1979, and references therein). These improvements in Fe I line formation parameters permit progress in diagnostic usage: for example Dravins et al. (1981) are able to study real convective motions rather than "turbulence" even from spatially-averaged data, with promising stellar ramifications.

However, a remaining concern in Fe I line formation is the influence of departures from Local Thermodynamic Equilibrium (LTE). The most detailed NLTE computations to date, by Athay and Lites (1972) and by Lites (1973), indicate large departures from LTE in solar Fe I. Nevertheless, these departures are neglected in many recent "classical" studies of the spatially-averaged solar spectrum (e.g. Gehlsen et al., 1978; Holweger et al., 1978; Blackwell and Shallis, 1979; Gurtovenko and Kostik, 1980). These studies generally admit variation only in element abundance and transition probabilities, in fitting parameters such as microturbulence, macroturbulence and collisional broadening fudge factors, and in the choice of atmospheric model. Such LTE analyses often support the LTE model photosphere of Holweger and Müller (1974) and its predecessor by Holweger (1967), by showing smaller variations in fitted quantities for these LTE models than for empirical NLTE models such as the HSRA (Gingerich et al., 1968).

In Fig. 1a we plot the temperature structure of the Holweger-Müller model (henceforth called HOLMUL), of the HSRA, and of the newest Vernazza et al. (1981) NLTE model for the quiet Sun (called VAL IIIC). Figure 1a shows the familiar discrepancies between the LTE and NLTE models, the HOLMUL model being appreciably hotter below $h=600$ km but ignoring the chromospheric temperature rise above this height. These discrepancies represent a long-standing problem which we address in this paper. Athay discusses them in his 1972 book (pp. 179–183) in terms of expected departures from LTE in typical lines fitted well by Holweger (1967) with his LTE model. Athay concludes that even if the electron temperature of Holweger's model is interpreted instead as an average NLTE excitation temperature, there is no ready explanation why this should exceed the HSRA temperature considerably in the upper photosphere. One would expect the reverse, because NLTE photon losses *depress* the ratio S^l/B (line source function to Planck function) below unity.

The properties of the LTE models are closely connected with departures from LTE in visual Fe I lines because the upper part of Holweger's (1967) model is largely based on the observed core intensities of strong Fe I lines near $\lambda=400$ nm (1 nm = 10 Å). The same holds for the HOLMUL model, which differs from Holweger's model only in the deep photosphere where it is based on the optical and near-infrared continuum. Holweger employed the observed equivalent widths of these blue Fe I lines to fix their oscillator strengths, chose his upper-photosphere temperature to reproduce their observed core brightness temperatures, connected this part of the model to the continuum-derived part through interpolation, and found that the result fits 900 solar lines rather

Send offprint requests to: R. J. Rutten

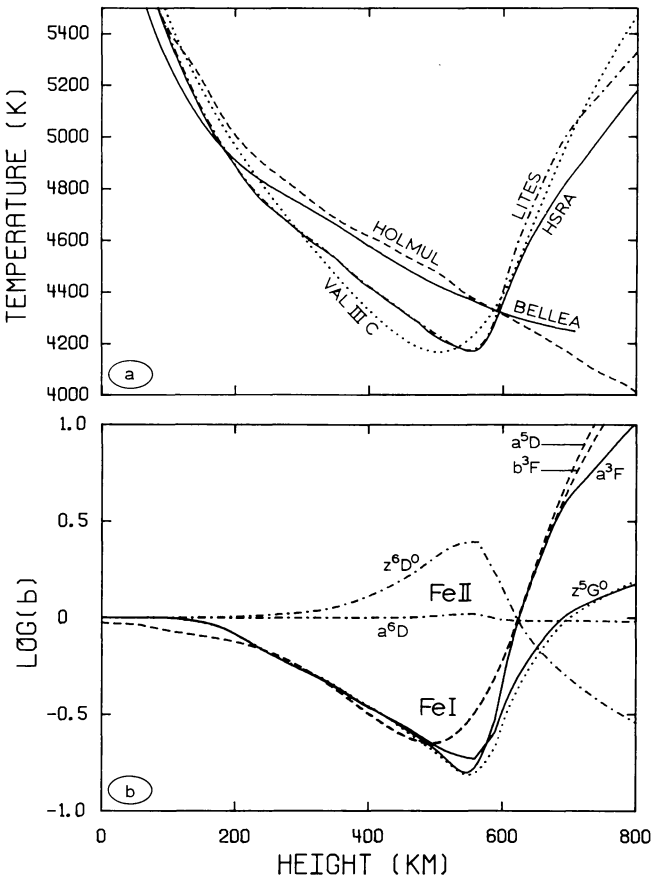

Fig. 1a and b. Published results of solar modeling. **a** Electron temperature versus height for various one-dimensional models of the solar atmosphere near its temperature minimum. The HSRA (solid), LITES (dot-dashed) and VAL IIIC (dotted) models are all empirical NLTE models. The HOLMUL model (dashed) is an empirical LTE model. The BELLEA model (solid) is a theoretical line-blanketed LTE-RE model. The height scale has its zero point at radial optical depth unity for $\lambda = 500$ nm. **b** Representative NLTE departure coefficients for Fe I and Fe II. Solid curves are results of Lites taken from Lites and White for Fe I levels a^3F and z^5G°. The dotted curve is a result for the same z^5G° level from another model atom. Dashed curves are results for the Fe I a^5D and b^3F levels taken from Vernazza et al. Dot-dashed curves are results for the a^6D ground level and the z^6D° excited level of Fe II taken from Cram et al.

well. Most classical LTE analyses since represent refinements of his impressive result. In contrast, Lites (1973) fitted high-quality profiles of 18 strong Fe I lines, observed center-to-limb by Lites and Brault (1972), very well with his HSRA-like model (Fig. 1a) using his NLTE computations. *Thus, the* LTE/NLTE *model discrepancies are connected to the extent and nature of* Fe I NLTE *effects.*

In this paper we discuss solar Fe I lines in the context of the large disparity between Holweger's LTE and Lites' NLTE description of their formation. We compare results of two classical LTE line-fitting analyses, made by one of us (Kostik). He fitted respectively the central depths and the equivalent widths of many medium-strong solar Fe I lines in the visible part of the spectrum, employing the HOLMUL model. We confront the differences between these two LTE fits with the NLTE predictions of Lites (1973), and we find disagreement. This we explore with numerical experiments in which we simulate LTE model building in Holweger's manner. We find that the disagreement is due to peculiarities of the HOLMUL model, of which we explain why it is as it is, and why it works so well for so many lines even though it is wrong. We so confirm quantitatively suggestions given in Paper I of this series by Wijbenga and Zwaan (1972).

II. Summary of NLTE Studies

Figure 1b contains representative results of Lites (1973), also found in Lites' thesis (1972), here taken from the detailed tables by Lites and White (1973). These publications are an extension of the analysis by Athay and Lites (1972). In addition, Fig. 1b contains recent results for Fe I taken from Vernazza et al. (1981), and also results for Fe II taken from Cram et al. (1980).

The NLTE departure coefficients b shown are defined differently for each of the three studies. They measure the population departure n/n^* where n is the actual population of the level and n^* the LTE population, normalized to the total number density of iron ($b=\beta$, Cram et al.), or normalized to the Fe II ground-state population ($b=b_c$, Lites), or normalized to the total Fe II population ($b=b_{\rm ion}$, Vernazza et al.). The preferable β convention was introduced in Paper I by Wijbenga and Zwaan (1972). The b_c convention is commonly employed in NLTE computer codes (e.g. Auer et al., 1972). The $b_{\rm ion}$ convention is the generalization of Menzel's original definition for hydrogen [Menzel and Cillié, 1937; cf. Jefferies, 1968, Eq. (6.3)]. Fortunately, the differences are small for solar Fe I because iron is about 90 % singly ionized throughout the photosphere, and about 70 % of the ions occupy the Fe II ground-state. Indeed, Cram, Rutten and Lites found the Fe II ground-state departure coefficient β to be unity throughout the atmosphere. We therefore neglect differences between β, b_c, and $b_{\rm ion}$ for Fe I here.

The results in Fig. 1b are based on different models of the solar atmosphere shown in Fig. 1a. Cram et al. use the HSRA. Lites' model (called LITES) differs slightly from the HSRA above $h=600$ km in its temperature and appreciably in its electron densities which are about three times larger, following Henze (1969). Vernazza et al. use their model VAL IIIC, which has chromospheric densities intermediate between the HSRA and the LITES model and a temperature minimum somewhat flatter and deeper located.

The solid curves in Fig. 1b are Lites' results for the levels a^3F and z^5G° of his "ground term model atom". The curve for a^3F shows the population behaviour of all levels of even parity up to b^3G at $\chi=3.0$ eV. The z^5G° level at $\chi=4.3$ eV is the highest computed level; its behaviour is shared by the upper levels of other strong lines. The dotted curve is Lites' result for the same z^5G° state from his "λ 4383 model atom" computation. It differs only slightly, indicating that the spread due to model atom setup choices is small. Vernazza et al. (dashed) use a 15-level model atom very similar to the reference atom of Athay and Lites. The two curves shown are for the lowest (a^5D) and highest (b^3F) levels tabulated by them. They agree very well with Lites' results, showing primarily the difference in model atmosphere. The two dashed curves are virtually the same, as are Lites' results for these even levels.

The Fe I departure pattern illustrates Athay and Lites' finding that most Fe I levels are *similarly* out of LTE above $h=100$ km. The departures are primarily due to imbalance in the radiative bound-free transitions, and they are for most levels virtually identical up

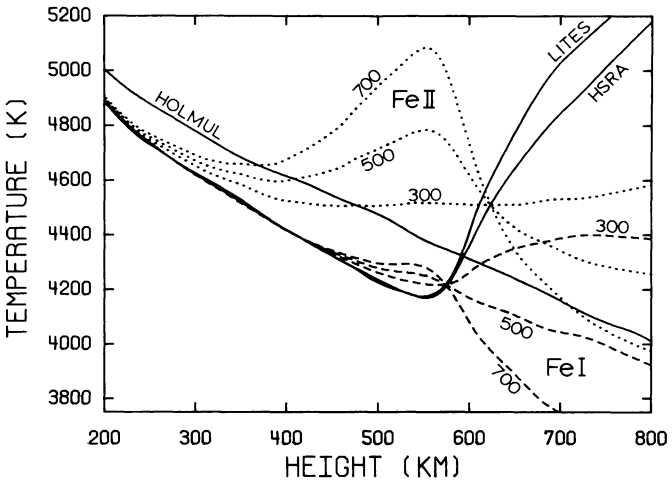

Fig. 2. Excitation temperatures against height for three wavelengths: $\lambda = 300$, 500, and 700 nm. Solid curves: electron temperatures of the indicated model atmospheres. Dashed curves: Fe I excitation temperatures derived from Lites' departure coefficients shown in Fig. 1b. Dotted curves: Fe II excitation temperatures derived from the departures coefficients of Cram et al. shown in Fig. 1b

to the temperature minimum. This is because the Fe I levels are well coupled, collisionally because they are numerous and close-lying, and radiatively because there are so many strong lines. The Fe I term diagram may be regarded as a closely-runged well-connected ladder, collectively populated through free-bound transitions from the Fe II ground term. At and below the temperature minimum there is overionization, hence underpopulation, because the ionizing ultraviolet radiation fields are characterized by higher radiation temperatures than the local electron temperature. Above the minimum the electron temperature quickly rises above the temperature of the ionizing radiation, resulting in rapidly increasing overpopulation. However, photon escape then causes upper-level depopulation relative to the lower level as shown in Fig. 1b. This divergence sets in at the height where the strongest lines with the particular level as upper level start feeling the presence of an optical boundary.

The departure pattern for Fe II is just the reverse: the upper and lower departure coefficients are *not* equal, and the upper level departures have a *maximum* at the temperature minimum. The coefficients shown in Fig. 1b (a^6D ground level and z^6D° excited level) are typical for Fe II because the low levels, again all of even parity, tend to be in Boltzmann equilibrium with the ground level, while many upper levels like z^6D° are fed by strong ultraviolet resonance-like transitions. Cram et al. found that strong radiation in the wings of these lines from the deep photosphere pumps the shared upper levels into overpopulation near the temperature minimum.

Figure 2 shows excitation temperatures derived from the departure coefficients in Fig. 1b for three wavelengths (see Wijbenga and Zwaan, 1972, for the conversion formulae). Changing the wavelength implies that the lower-level excitation energy is varied while the upper remains fixed. Because all available low levels are even and strongly coupled in both Fe I and Fe II, Fig. 2 is representative for *all* lines with upper levels like z^5G° and z^6D°, thus for most Fe I and Fe II lines. Their level-by-level population equality leads to source function *in*equality: the wavelength dependence illustrates that line source function departures *increase* towards longer wavelengths for given population departures [this follows directly from the approximation $S_\nu^l = (\beta_u/\beta_l) B_\nu$; see also Mihalas, 1978, p. 404]. Both the Fe I and the Fe II excitation temperatures do not follow the chromospheric rise of the electron temperature. At the temperature minimum and below, the Fe II excitation temperatures are appreciably raised above the electron temperature while the Fe I excitation temperatures are close to it. Of course, only the strongest lines, which are mostly near $\lambda = 300$ nm, are sensitive to the excitation departures because they, in fact, set them. For example, there is no Fe II line near $\lambda = 700$ nm strong enough to feel the high peak of the $\lambda = 700$ nm Fe II excitation temperature. (Note, however, that this situation changes at the extreme limb. Figure 2 explains why Fe II lines turn into emission *inside* the limb, while Fe I lines do not.)

Finally, Fig. 2 demonstrates that the HOLMUL electron temperature can indeed not be interpreted as representing an average NLTE excitation temperature for Fe I lines.

We summarize these results: up to the temperature minimum the Fe I lines have Boltzmann equilibrium but increasing Saha departures, while Fe II lines have increasing Boltzmann departures. The line *source functions*, which depend on the departure coefficient ratio β_u/β_l of the upper and lower levels, should generally be in LTE for Fe I, and out of LTE for Fe II. In contrast, the line *opacities*, which scale with β_l, should be equal to the LTE values for Fe II but appreciably smaller for Fe I. Above the temperature minimum the Fe I opacity departures reverse, and the Fe I and Fe II line source functions drop below the Planck function due to photon losses.

III. Input Data: Δ Values

The data used in this study are the results of two LTE fitting analyses of medium-strong Fe I lines performed at Kiev. Both analyses employed the HOLMUL model. In the first (Gurtovenko and Kostik, 1980, 1981) the *central intensities* of 865 Fe I lines at the center of the solar disk were fitted by varying their oscillator strengths, the iron abundance, the micro- and macroturbulence and an enhancement factor to the classical Van der Waals damping constant. For a subset of 385 of these lines (unblended lines for which published equivalent widths were available at Kiev) a second procedure was performed, fitting the *equivalent widths* (Gurtovenko and Kostik, 1982; their set of 360 lines was extended with 25 lines for this analysis). The ratios of these line-depth (gf_d) and line-area (gf_w) fitting oscillator strengths are our input data; their logarithmic differences $\Delta = \log(gf_d) - \log(gf_w)$ are shown in Fig. 3a as a function of upper-level excitation energy. The differences Δ are centered on zero, and their spread is remarkably small: $\bar{\Delta} = 0.0 \pm 0.17$, where the error indicates the 95 % confidence limits per sample. The high consistency between these two fits demonstrates once more that visual Fe I lines can be fitted well assuming LTE and the HOLMUL model.

Figures 3b and 4 complete the display of the input data. Figure 3b shows the gf_d values against upper-level excitation energy. We do not show a similar plot of the gf_w values because it is nearly the same. Figure 4 shows the Grotrian diagram of the 385 lines. Together, these figures illustrate an important selection effect which affects all studies limited to "nice" Fe I lines in the visible part of the spectrum: only at high excitation are lines included with large transition probability (gf of order unity). For example, all resonance lines, which have upper levels between $\chi = 3$ eV and $\chi = 5$ eV, are absent because they are in the near ultraviolet. The only

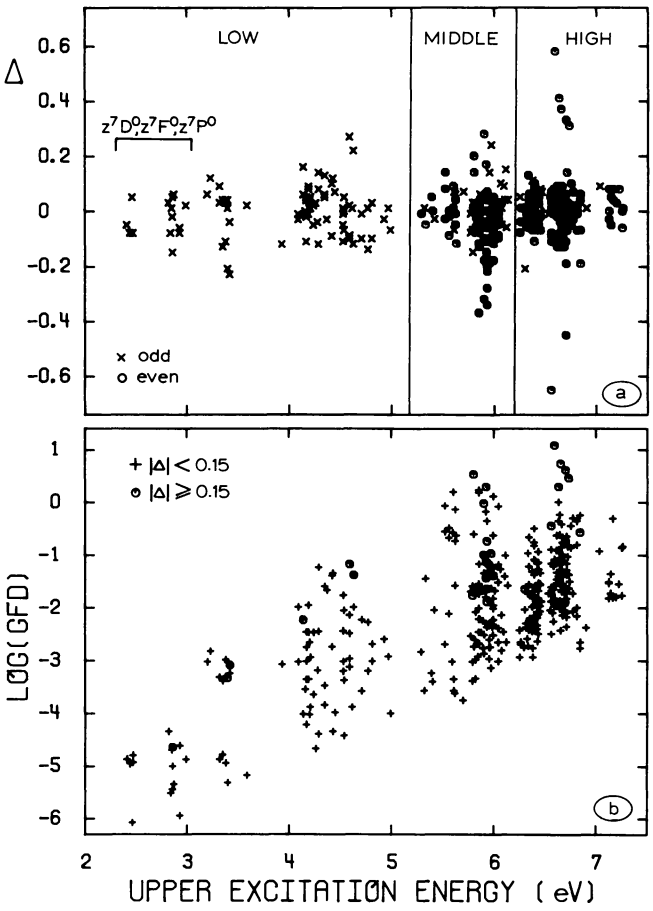

Fig. 3a and b. Input data of this study. **a** Δ against upper-level excitation energy for 385 Fe I lines. Δ = the difference log (gf_d) – log (gf_w), where gf_d is the oscillator strength fitting the observed line-core depression and gf_w is the oscillator strength which best fits the observed equivalent width. $\Delta > 0$ implies that a line is too deep for its area when modeled with the HOLMUL model. The crosses are for lines with upper levels of odd parity. The circles are for even-parity upper levels. The lowest levels are indicated with their designations; these are special "semistable" levels, which feed only weak intercombination lines. **b** The logarithm of the gf_d oscillator strengths against upper-level excitation energy. The circles are lines with values of $|\Delta| \geqq 0.15$, of which there are 32

lines to the ground level present are the weak intercombination lines of multiplets 1, 2, and 3. Many other UV multiplets and many principal lines of other multiplets are also missing; Fig. 3b shows that the sampling includes downward transitions of large probability *only* above $\chi = 5$ eV. These high-excitation lines are comparatively weak due to the small Boltzmann factors. The decrease of the Boltzmann factor also sets the lower boundary of Fig. 3b, at which lines become too weak to be easily measured.

IV. Analysis

a) Specific Lines and Excitation Classes

We first consider the question whether extreme Δ values are an individual property of specific lines. Plots of Δ against line strength per multiplet generally show smooth relations, indicating that unnoticed blends, which would produce jumps in Δ for affected lines, are not causing the extreme Δ values. The 32 lines with $|\Delta| \geqq 0.15$ are indicated by circles in Fig. 3b and by dashed transitions in Fig. 4. These diagrams, and comparison with the strong-line Fe I term diagram of Moore and Merrill (1968), indicate no preference of extreme Δ values for specific terms, and that there is no reason to suspect pumping of particular levels. Also, the magnetic lines of high Landé factor g (λ 525.02, λ 572.45, λ 617.33, and λ 684.27), and the velocity lines with $g = 0$ (λ 512.37, λ 557.61, and λ 709.04) do not show special Δ behaviour, in agreement with the result of Stenflo and Lindegren (1977). We therefore discuss the average Δ patterns of our whole sample.

We split the data into three line classes indicated in Fig. 3a: "low" lines (upper levels below $\chi = 5.2$ eV; 88 lines), "middle" lines (upper levels between $\chi = 5.2$ eV and $\chi = 6.2$ eV; 108 lines), and "high" lines (upper levels above $\chi = 6.2$ eV; 189 lines). These line classes are suggested by the distributions in Fig. 3. Note that it is better to group Fe I lines according to their upper levels than to their lower. Upper-level grouping is a classification of *potential* excitation departures which, if present at all, will show up primarily in lines that are the strongest available of each group. A plot of Δ against lower-level excitation energy is less clearly dividable, and, for example, mixes the intercombination multiplets 13 and 14 together with the permitted multiplets 15 and 16 at $\chi = 1$ eV.

We first discuss the low lines. These are of two types. The lines with upper levels below $\chi = 3$ eV are all from the special z^7D°, z^7F°, and z^7P° levels called "semistable" by Athay and Lites. These levels have no permitted downward transitions at all but only intercombination lines of small oscillator strength, namely multiplets 1, 2, 3, 12, 13, and 14. In contrast, the higher odd levels possess many resonance-like downward transitions of large probability, both permitted and intercombination lines. However, our low lines sample only much smaller oscillator strengths; Lites' results predict LTE excitation for all of them because they are all weaker than the near-ultraviolet lines that maintain the excitation balance up to the temperature minimum. Lites' departure coefficients for the three semistable levels are also equal to those of the ground level and the other low even levels up to the temperature minimum, implying that *all* low intercombination lines have LTE excitation, including the strongest (which are not in our sample). Their photon losses upset the collisionally maintained balance only in the chromosphere, where the coefficients of the semistable levels do diverge from the coefficients of the even levels. This behaviour is analogous to the LTE excitation of the well-known Mg I λ 457.11 intercombination line. We therefore group these lines together with the permitted low lines; Fig. 3a shows indeed no difference between them.

Lites' results do not cover the lines with upper levels above $\chi = 5.2$ eV, which make up our "middle" and "high" classes. Athay and Lites discuss a computation for one high level, at $\chi = 6.4$ eV. Its departure coefficient equals that of z^5G° until $h = 300$ km and then drops below it, due to photon loss in a downward transition which has optical depth unity near the temperature minimum. At that height the upper-level departure is twice the lower-level departure. Similar behaviour is shown by Lites' computation for the λ 523.29 magnetic line (upper level e^7D at $\chi = 5.3$ eV) even while he needs unusually high collisional coupling to fit that line. These two examples should be representative for most high-excitation levels because they have much weaker "strongest" downward transitions than the lower odd levels which feed the resonance(-like) lines.

We conclude that *only* our high lines of large oscillator strength may show excitation departures, because only they are the

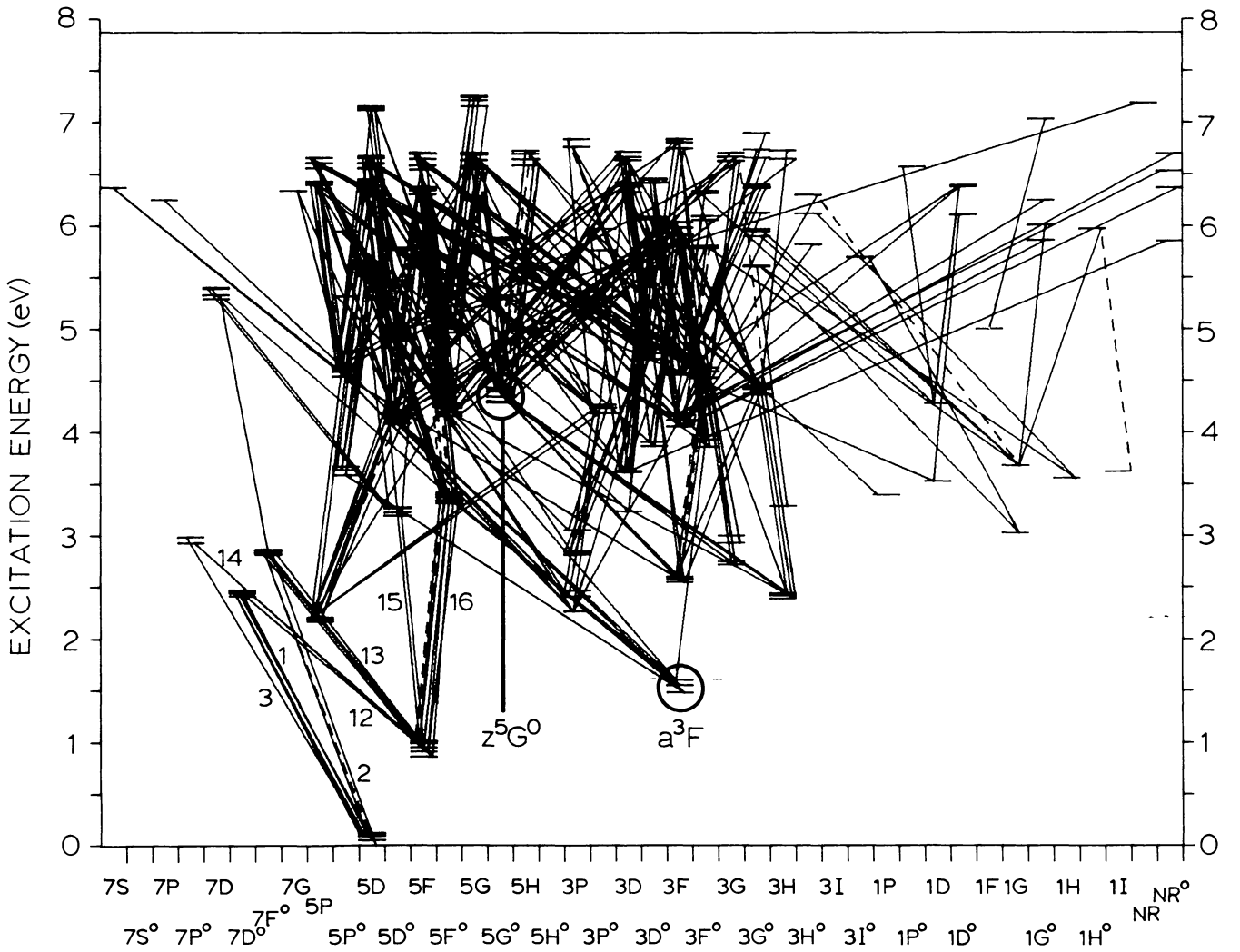

Fig. 4. Fe I term diagram. The transitions with $|\Delta| \geqq 0.15$ are dashed. Level designations and excitation energies have been taken from Moore (1959). The intersections of transitions and levels are shifted progressively to the right for increasing quantum number j. Levels with a number designation in Moore (1959) are combined into the terms NR and NR° at right. The circles identify the a^3F and z^5G° levels used as representative. The special low-probability intercombination multiplets are at the lower left

strongest transitions available from their upper levels. Such lines should have excitation temperatures *below* the electron temperature. In contrast, Lites' results predict appreciable opacity departures throughout the upper photosphere, virtually equal for *all* lines of our sample, due to the NLTE ionization.

b) Interpretation of Δ as NLTE *Departure Coefficient*

Figure 5 shows Δ against line strength. For each line class it shows a pattern, with increasing line strength, of a slight decrease from $\Delta = 0$ followed by an increase to $\Delta > 0$. This pattern mimics the Fe I log (b) pattern shown in Fig. 1b. There is indeed reason to interpret Δ as an observational measure of the departure coefficient β_l of the lower level for each line. This is because equivalent widths are less sensitive than central intensities to departures from LTE. The departures are smaller in the deep layers where weak Fe I lines are formed and where the line wings are formed which contribute most to the equivalent widths of stronger Fe I lines, than they are in the higher layers where the line cores are formed. If we may neglect departures from LTE in the fits of the equivalent widths, and if the model atmosphere, the turbulences, the damping etc. are all correct, then the differences Δ measure errors due to the assumption of LTE for the line cores only. If in addition the line source functions equal the Planck function at the formation height of the line cores, as predicted above for all low lines and most middle and high lines, then the Δ values would describe empirical NLTE adjustment factors to the local line opacity, expressed as the changes of the oscillator strengths needed to reconcile the computed LTE profiles with the observed line cores. Because line opacity is proportional to the product of the oscillator strength and β_l, the Δ values would thus be *identical* to the neglected NLTE line opacity corrections log (β_l) at the heights of formation of the line cores.

To enable comparison of the observed Δ and predicted log (β_l) patterns we have computed the mean height of formation at line center for each line, defined as usual by

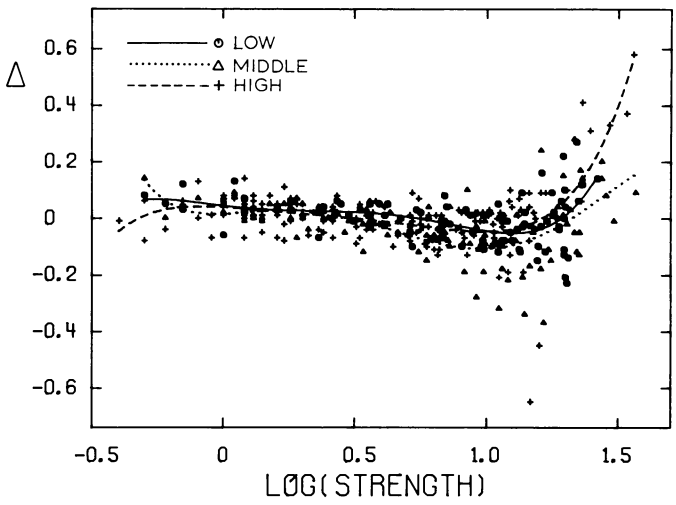

Fig. 5. $\Delta = \log(gf_d) - \log(gf_w)$ against log (strength) for 385 Fe I lines, divided into three excitation classes as indicated. The line strength is the reduced equivalent width (W/λ 10^6) in Fraunhofer units taken from Moore et al. (1966). The curves are least-square polynomial fits for each class

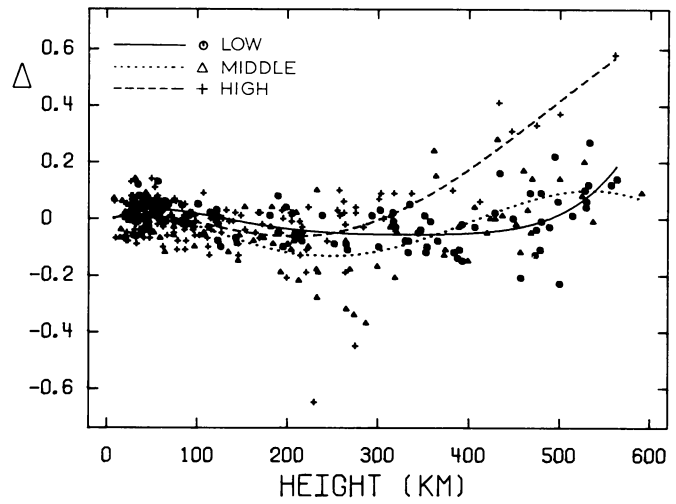

Fig. 6. $\Delta = \log(gf_d) - \log(gf_w)$ against height of formation for 385 Fe I lines, divided into three excitation classes as indicated. The height scale measures mean height of formation of the line core when computed with the gf_d oscillator strengths for the HOLMUL model. The solid, dotted, and dashed curves are least-square polynomial fits to the low, middle and high classes, respectively

$$\langle h \rangle = \int_0^\infty hj \exp(-\tau) dh \Big/ \int_0^\infty j \exp(-\tau) dh,$$

where j is the total emission coefficient per cm^3 and τ is the total optical depth, at height h; $j \exp(-\tau)$ is the contribution function to the emergent intensity. Figure 6 shows the result. Compared with Fig. 5, the high-excitation lines (pluses) have moved to the left because these lines are formed deeper than low-excitation lines of similar strength. All line cores are formed below $h = 600$ km.

Interpreting the Δ values as lower-level departure coefficients thus makes their patterns directly comparable to Lites' predictions in Fig. 1b. We should find differences between these two graphs only, if any, for the strongest high-excitation lines. The high lines (pluses and dashed fit) deviate indeed above $h = 350$ km from the low and middle lines. The latter, however, show large disagreement with the NLTE predictions. The solid and dotted curves, which are fits to the low and middle lines respectively, barely differ from $\Delta = 0$ instead of reaching the predicted minimum of $\Delta \approx -0.7$ near $h = 500$ km in Fig. 1b.

This striking disagreement indicates that either Lites' NLTE description of solar Fe I line formation is entirely wrong and that the true Fe I ionization departures are very much smaller, or that the empirical LTE fitting procedures have hidden the true NLTE departures in other parameters. A candidate for such a NLTE-masking parameter is the HOLMUL model itself, because it is *based* on similar LTE fitting of observed Fe I line cores. Thus, the disagreement leads to questioning the LTE assumption underlying the HOLMUL model itself. Another motivation to this reappraisal is that the existence and location of the minimum in the electron temperature are now so well established (see Vernazza et al., 1981) that the conflicting HOLMUL model, *and its success in line fitting*, require explanation.

c) *Experiments in* LTE *Model Building*

We turn now to schematic numerical experiments studying the influence of Fe I NLTE on Holweger's model-building procedure. Let us assume the validity of the LITES model and the concomitant Fe I departure coefficients, turbulence and damping formalism used by Lites (1973), that is: let us assume that Lites' NLTE interpretation of solar Fe I lines is entirely correct. Our experiments then consist of computing schematic iron lines with oscillator strengths iteratively set to produce equivalent widths of $W = 2, 4, 6, 8, 10, 15, 20, 25, 30, 40, 50, 75, 100$, and 125 pm (1 pm = 10 mÅ), in a grid of three wavelengths ($\lambda = 400$, 550, and 700 nm; 1 nm = 10 Å) and three lower-level excitation energies ($\chi = 1.5$, 3.0, and 4.5 eV). This grid covers our Fe I lines and also all Fe I lines used by Holweger. We use a FORTRAN version of the line synthesis program described by Rutten (1976); following Lites, we employ Brückner's (1971) formalism for collisional damping by neutral perturbers, in our case using Irwin's (1979) approximation to it, and we similarly include quadratic Stark broadening, temperature-dependent partition functions, macroturbulent smearing by 1.0 km s^{-1}, and Lites' height-dependent microturbulence.

For the level population departure coefficients we choose Lites' results for a^3F and z^5G°, shown in Fig. 1b, for all grid categories. Our low and middle line classes consist of blue and green lines which are well represented by the a^3F and z^5G° departure coefficients used for our $\chi = 1.5$ eV and $\chi = 3.0$ eV grid categories. For example, the ($\chi = 1.5$ eV, $\lambda = 400$ nm) category describes multiplet 41 and the very similar multiplets 42, 43, 45 etc., which provide resonance-like lines in the visible part of the spectrum; multiplets 41 and 43 were used by Holweger to set the upper part of his model. The ($\chi = 3$ eV, $\lambda = 500$ nm) category is representative for upward transitions from levels such as a^5P, a^3D, a^3H, b^3F, and b^3G of which the departures are all equal to those of a^3F. For our high lines Lites' work does not provide representative upper-level coefficients. The computation for one level at $\chi = 6.4$ eV by Athay and Lites mentioned above indicates that our use of the a^3F and z^5G° departure coefficients produces proper opacity departures up to $h = 600$ km, and proper source function departures (i.e. none) up to $h = 300$ km for such lines.

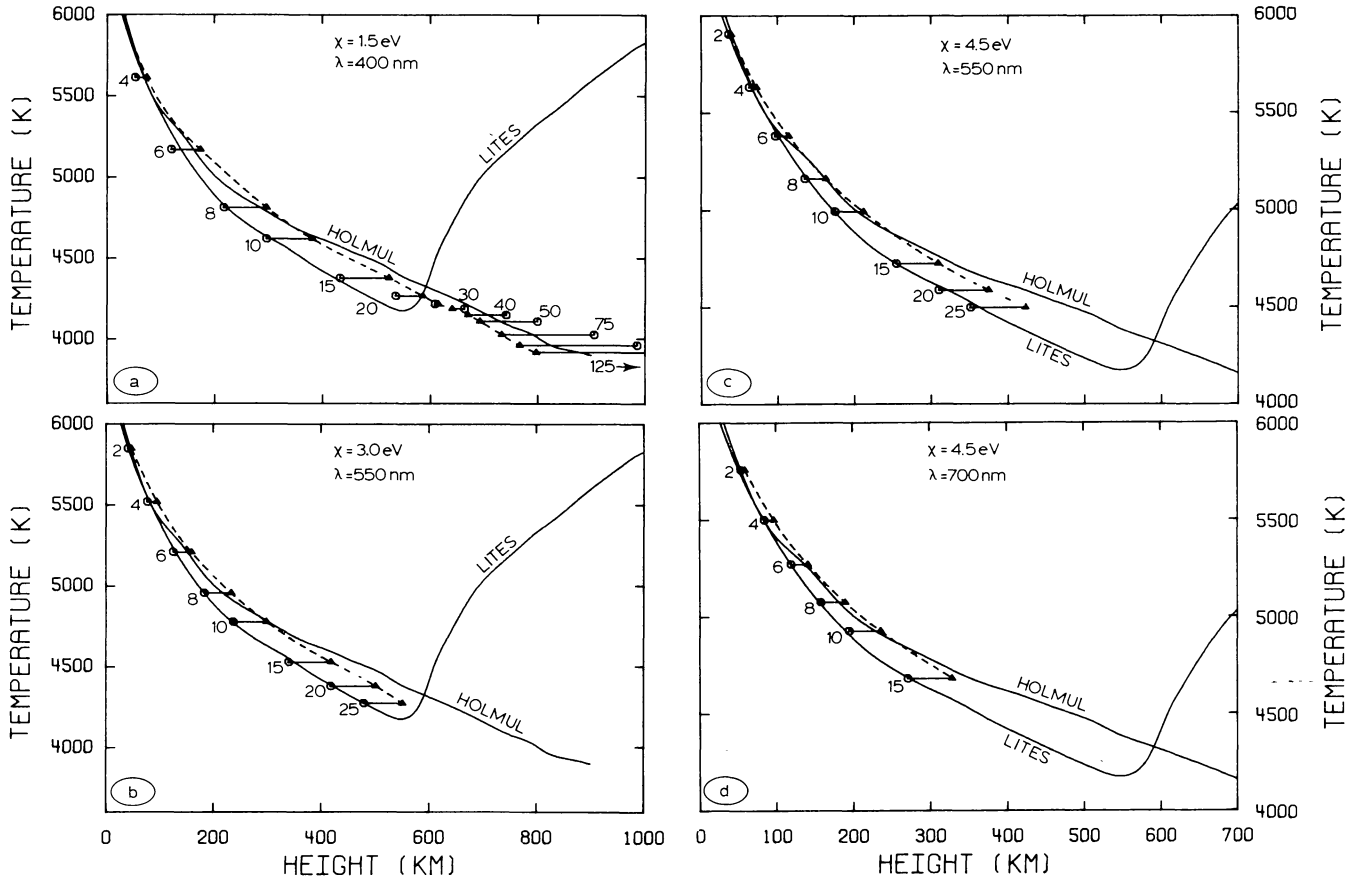

Fig. 7a–d. Results of numerical experiments showing the influence of the neglect of departures from LTE on Fe I lines, for the indicated combinations of lower-level excitation energy and wavelength. The solid curves are the electron temperatures of the LITES and HOLMUL models. The circles are line-center brightness temperatures for lines of the indicated equivalent widths (pm) at their heights of formation, both computed from Lites' NLTE results. The triangles are the same brightness temperatures, but shifted to the line-center heights of formation derived assuming LTE. The dashed curves connecting the triangles may be regarded as a first iteration in a model-building procedure from Fe I line cores in Holweger's fashion

Our Holweger-like model building proceeds as follows. We convert the central intensity of each synthesized profile into brightness temperature. Since we assume Lites' modeling to be correct, these represent the "observed" brightness temperatures of our schematic lines. We then recompute the lines again with the LITES model and with identical parameter values, except that the NLTE departure coefficients are replaced by unity throughout the atmosphere. We plot the "observed" line-center brightness temperature from the NLTE computation against the line-center height of formation from the LTE computation. This plot shows the run of the excitation temperature which one derives from observed line core brightnesses *if they are interpreted on an* LTE *opacity scale*, in precisely the inverse Eddington-Barbier method of model building used by Holweger.

Figure 7 shows results. In each panel the circles denote the computed central intensities at disk center converted into brightness temperatures, at the height of line-center formation from the Lites-like NLTE computation. The numbers specify the quivalent widths of the lines in pm, up to the largest value observed in the solar spectrum for each grid category. The triangles denote the same line-center brightness temperatures, but shifted horizontally to the height of formation of the same lines computed without NLTE departures. This shift shows the NLTE opacity effect. The shift is to the right ($h<600$ km) or to the left ($h>600$ km) depending on lower-level underpopulation or overpopulation as felt by the line core, respectively.

The circles follow the LITES electron temperature as long as $\beta_l=\beta_u$, apart from slight shifts where the run of the model temperature has large curvature so that its weighting by the intensity contribution function results in breakdown of the Eddington-Barbier relation; these shifts are largest in the blue. At larger heights the circles follow the NLTE excitation temperatures shown in Fig. 2, also weighted by the intensity contribution function.

The triangles follow the circles, but displaced over the inverse NLTE opacity departures. We have connected the triangles by dashed curves. Each curve represents a simulated Holweger model for its grid category. Below $h=600$ km the opacity shifts result in apparent brightness temperature excess. Above $h=600$ km the electron temperature rise is not seen at all by the lines. The dashed

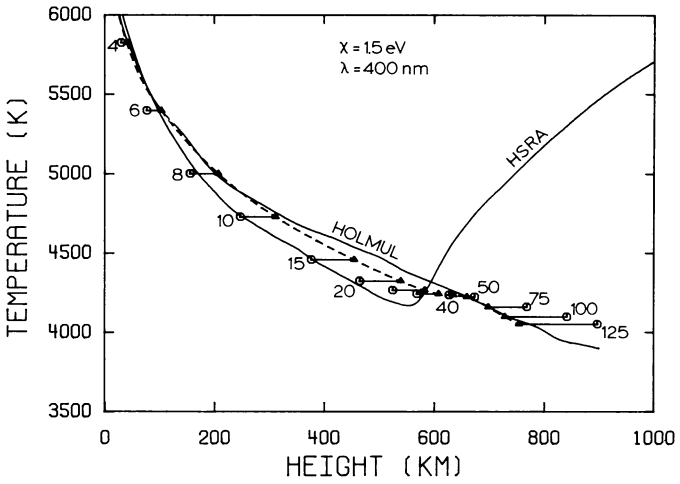

Fig. 8. Results of experiments as in Fig. 7, employing the HSRA model with Lites' Fe I NLTE results

curves are very similar for all grid categories, and they are all remarkably close to the HOLMUL model. Together, they cover the *whole* range of Holweger Fe I lines, in strength, wavelength and excitation energy. Thus, our numerical experiment results for *all* Holweger Fe I lines in NLTE brightness temperatures which, *when they are placed on* LTE *opacity scales*, are closely mimicked by the HOLMUL electron temperature.

Note that the dashed curves represent a first approximation to Holweger's procedure. In further simulation, we should equate the electron temperature to the dashed curve, and compute new densities obeying hydrostatic equilibrium. This would reduce the NLTE-to-LTE opacity shifts above $h = 600$ km; they would also be reduced slightly because deletion of the chromospheric temperature rise increases the relative LTE Fe I population.

In Fig. 8 we investigate the model dependency of our experiment. The LITES model differs mainly from the HSRA and similar models in its chromospheric densities. We have repeated the experiments of Fig. 7 using the HSRA instead; the ($\chi = 1.5$ eV, $\lambda = 400$ nm) result is shown. The lines are formed deeper than in Fig. 7a, but the dashed curve remains similar.

The close correspondence of the dashed curves and the HOLMUL model leads to the following conclusion: *accepting Lites'* NLTE *modeling of the solar* Fe I *spectrum implies that Holweger's* LTE *model-building procedure leads inevitably to a* HOLMUL-*like model*. The HOLMUL model thus achieves NLTE-*masking*: it hides the NLTE departures of Fe I lines in its temperature structure. The NLTE-masking is achieved primarily through setting a spurious height scale (or τ^c_{500} scale) by neglecting lower-level population departures, and in addition by setting the electron temperature above $h = 500$ km to mimic the opacity-shifted excitation temperatures of the strong Fe I lines near $\lambda = 400$ nm.

The small spread between the various dashed curves in Fig. 7 indicates that this NLTE-masking works remarkably well for all grid categories. The dependence of the dashed curves on excitation energy, which mostly affects the heights of formation and thus the opacity shifts, results in a slight lowering (compare Fig. 7b and c). The main change toward longer wavelengths (Fig. 7c and d) is a slight steepening resulting from smaller Eddington-Barbier offsets due to lesser Planck function curvature. These changes are so small that the HOLMUL model represents all dashed curves very well.

The NLTE-masking is thus effective for *all* visual Fe I lines. The reason for this fortunate result is that the opacity departures, which influence all lines throughout the upper photosphere, are nearly identical for all lines, while of all visual lines only the strongest triplet-system lines feel source function departures; these lines are all near $\lambda = 400$ nm and are well represented by a single excitation temperature. Note also that the latter happens to vary so slowly with height that it is indeed recovered by Holweger's inverse use of the Eddington-Barbier relation, without curvature offsets.

d) Interpretation of Δ as NLTE-*masking Indicator*

We now turn back to the Δ patterns of Fig. 6. It is now clear that Δ should not be interpreted as measuring real NLTE departure coefficients, but rather as measuring failures of the LTE fitting procedures to reproduce Fe I lines as well as possible with the HOLMUL LTE model. Thus, Fig. 6 indicates the quality of the HOLMUL NLTE-masking. The small values of $|\Delta|$ confirm that the HOLMUL model achieves its implicit NLTE corrections remarkably well.

The HOLMUL NLTE-masking is most effective for the low and middle lines, for which the least-square fits (solid and dotted curves) are close to zero everywhere. This is not surprising because the model was build from such lines. The remaining errors need in fact not be masking errors; the slight dips in Δ may be due to underestimation of the collisional damping. The value of $1.3 \times \gamma_{vdW}$ used by Gurtovenko and Kostik (1982) seems somewhat small in view of theoretical and recent experimental work (Brückner, 1971; Deridder and van Rensbergen, 1976; O'Neill and Smith, 1980). Too small damping parameters lead to too large gf_w fits, thus to too small Δ values, for lines with damping wings. The resulting strong-line dip in the three curves should be at similar equivalent width rather than at similar formation height; this is indeed shown by Fig. 5 in which the three curves are very similar.

The high lines show a significant mean increase of Δ with height above $h \approx 350$ km (dashed curve; its 95 % confidence limits are typically $\delta\bar{\Delta} = \pm 0.06$). This implies that their opacity-shifted source functions drop below the HOLMUL Planck function at this height, and thus that their true line source functions drop below an HSRA-like Planck function above $h \approx 300$ km. This corresponds very well with the prediction for the $\chi = 6.4$ eV level by Athay and Lites quoted above.

We conclude that only our strongest high lines show incomplete NLTE-masking. This agrees with our inferences above that only these lines should show excitation departures differing from the excitation departures of multiplets 41 and 43. Thus, the patterns of Fig. 6, while inconsistent with our earlier $\Delta = \log(\beta_l)$ interpretation, are entirely consistent with our NLTE explanation of the HOLMUL model. In fact, they support Lites' NLTE representation of the solar Fe I spectrum even quantitatively. The closeness of the HOLMUL model to the dashed curves in Fig. 7 implies that good LTE fits of Fe I lines with the HOLMUL model *require* Lites-like population departures for reconciliation with the well-defined existence of a temperature minimum as it is present in the more realistic HSRA and VAL IIIC models. The very small values of $|\Delta|$ for the low lines in Fig. 6 therefore *show* that the LTE-to-NLTE opacity corrections necessary to reduce the HOLMUL model to an HSRA-like model are indeed of the size found by Lites. They so extend Lites' good fit of the strong Fe I lines to the weaker Fe I lines. *We infer that the high quality of the* LTE *fit actually supports the size as well as the presence of the* NLTE *departures*!

V. Discussion

a) Lites' Results Compared with Other Studies

We first compare Lites' results, on which our NLTE explanation of the HOLMUL model is based, with other analyses of solar Fe I. The only other comparable Fe I computations are those by Vernazza et al. (1981). Unfortunately, we cannot repeat our experiments for their model because they list only the departure coefficients of the low even levels, which have no radiative transitions between them. However, the good correspondence with Lites' results for these levels (see Fig. 1b) supports the earlier work.

An empirical study of interest is the one by Smith (1974), which is commonly misquoted as indicating that LTE is a valid assumption for solar Fe I lines. It does not, because it is restricted to the excitation equilibrium only (as stated carefully in the paper). Smith performed an analysis much like our own, comparing observed central intensities of visual lines with LTE predictions. However, he used the HSRA model and employed Athay and Lites' NLTE opacities. Thus, Smith tested *only* the line source function departures, while accepting Athay and Lites' results for the ionization balance which sets the opacity scales. He finds excellent agreement of the observed and computed line core intensities up to the temperature minimum, implicitly confirming the importance of the NLTE opacity corrections required to fit the weaker Fe I lines with the HSRA.

Smith also confirms the existence of excitation departures above the temperature minimum. He finds that these are only 50–60 % of those of Athay and Lites. However, this result may be sensitive to his incorrect use of a single depth-independent damping constant set equal for all lines. This simplification, which also affects Smith's (1974) similar study for Arcturus, may explain why he finds large disagreement between observed and computed lines when using Holweger's LTE model, in conflict with Holweger's own work and the Kiev fits used here.

We conclude that there is no evidence of any major shortcoming in Lites' work, and so we do not agree with the comment given by Blackwell et al. (1980) on the analysis by Athay and Lites that no general conclusions on Fe I NLTE have yet been drawn. In contrast, the success of their own classical studies, of those by Holweger and collaborators, and of the Kiev fits discussed here, in reproducing solar Fe I lines assuming LTE and the HOLMUL model should in fact be intepreted as further confirmations of Athay and Lites' and Lites' NLTE modeling of the solar Fe I spectrum.

b) Extensions to Lites' Work

A possible minor shortcoming in Lites' analysis is his assumption of complete frequency redistribution over the line profiles, because coherency effects have in the meantime become familiar complications for other spectra (see Milkey, 1976). Fe I has many pathways for interlocking to destroy the coherency made possible in many lines by the existence of so many metastable levels, and partial redistribution (PRD) effects may therefore indeed be negligible. Nevertheless, there are two empirical indications of slight PRD effects. These are Lites' problem in fitting the inner wings of the strong lines, and Rutten and Stencel's (1980) observation of line-wing emission in multiplet 4 lines seen just inside the limb. This pattern mimics the Ba II λ 455.40 PRD profile near the limb (Rutten and Milkey, 1979). Similar patterns are also indicated for many near-ultraviolet Fe I lines in the tabulation of the spectrum of the extreme limb by Pierce (1968). Thus, PRD effects seem to exist; they may also explain Lites' problem in fitting the limb darkening of the cores of five strong lines. However, they will probably not affect the iron population equilibria by much.

Another point of interest is to study population departures of high-excitation Fe I levels in more detail. The computations for a $\chi = 6.4$ eV level by Athay and Lites and for the e^7D level at $\chi = 5.3$ eV of Lites' "magnetic lines atom" predict that their departure coefficients drop below the lower level departures above $h = 300$ km. One would expect similar behaviour for all high levels with weak but probable downward transitions, unless even the strongest lines are so weak that the continuum dominates (Lites, private communication); one then expects fulfillment of the frequent assertion (e.g. Jefferies, 1968; Rogerson, 1969; Smith, 1974) that the high levels should be in equilibrium with the continuum which has $\beta = 1$. In that case the high-level departure coefficients should fill in rather than deepen the dip shared by the lower levels in Fig. 1b. Note that in both cases the excitation is out of LTE already above $h = 300$ km. A third case, equality of the departure coefficients, is advocated by Ruland et al. (1980). They argue that the neglect of the numerous high-excitation levels of Fe I and the neglect of collisions with hydrogen atoms lead to spurious departures in the computed excitation equilibrium.

We conclude that, although the outward rise of the dashed curve in Fig. 6 supports the results of Athay and Lites, this question requires further model computations. We expect, however, that the ionization balance will not change much when the number of high levels and their collisional coupling rates are increased, because of the fact, noted by Athay and Lites, that most high Fe I levels ionize to higher Fe II parent levels than the Fe II ground level. The excitation balance may then be set by the strongest upper-level *group* rather than per upper level; empirically, the excitation balance is best studied using lines of long wavelength, observed towards the limb (see Fig. 2).

c) NLTE *Masking for Other Spectra*

We now turn to other spectra than Fe I. Opacity departures will similarly influence Fe I-like spectra, e.g. Ti I. In general, all minority species with complex spectra and NLTE ionization equilibria will be put on a wrong height scale when interpreted in LTE, resulting again in effective NLTE-masking by an opacity-shifted model. This suggests why the HOLMUL model works well for many atomic lines.

In addition, the HOLMUL model achieves NLTE masking to some extent for lines of majority metal species. We demonstrate this for Fe II. The Fe II departure coefficients shown in Fig. 1b lead to the highly suprathermal excitation temperatures of Fig. 2. These describe typical Fe II line formation; in this case there are no NLTE opacity shifts. The HOLMUL model lies closer to the excitation temperatures than the HSRA model; thus, the HOLMUL model again hides excitation departures at least partially in its temperature structure. Note that the only strong Fe II lines employed by Holweger are those of multiplet 42 near $\lambda = 500$ nm, and that these have shallower cores than computed from his model, in accordance with Fig. 2. The excitation temperatures of the stronger Fe II lines at shorter wavelengths are better mimicked. Thus, the HOLMUL model turns out to be functioning reasonably well for both Fe I and Fe II. This explains why Blackwell et al. (1980) find better agreement for the HOLMUL model than for the VAL IIM model (Vernazza et al., 1976), when comparing Fe I and Fe II assuming LTE. With the VAL IIM or similar models there *must* be

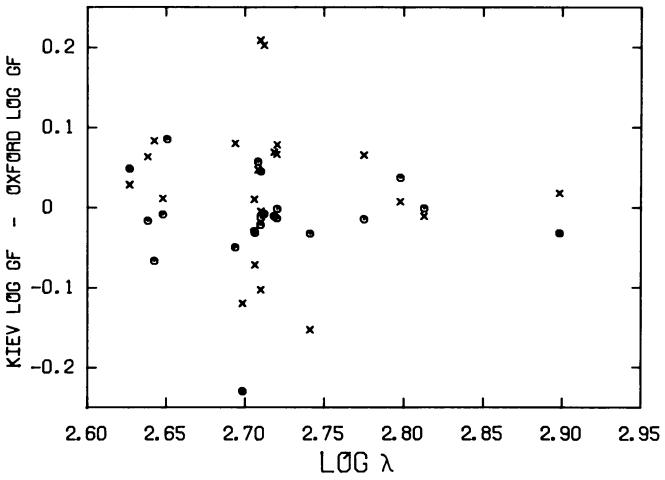

Fig. 9. Differences in solar and laboratory oscillator strengths for all lines of overlap against log (λ) with λ the wavelength in nm. Circles: solar values gf_d derived from central depths. Crosses: solar values gf_w derived from equivalent widths

divergence in LTE-fitted abundance values: the Fe I lines are then located too high, requiring too low an abundance, whereas the Fe II lines are assigned too low excitation temperatures, requiring too high an abundance. This divergence for the VAL IIM model does not demonstrate the superiority of the HOLMUL model, as they suggest, but rather the latter's success in hiding NLTE departures for both Fe I and Fe II. That this masking is less good for Fe II is displayed by the wider "neck" in their Fe II diagrams. The divergence indicates that even Fe I equivalent widths are sensitive to departures from LTE. This topic will be discussed along with the Fe I curve of growth in the next paper in this series (Rutten and Zwaan, 1983).

d) Comparison with Laboratory gf-values

The quality of the NLTE-masking by the HOLMUL model is confirmed once more by Fig. 9, which shows differences between the gf_d and gf_w values and the precise laboratory measurements by Blackwell et al. (1979) and Blackwell et al. (1979), to which the gf_d scale was normalised by Gurtovenko and Kostik (1981). All lines present in the Oxford data that are also present in the Kiev gf_d list (22 lines) and in the extended Kiev gf_w list (21 lines) are shown. The mean offset between the two sets reflects the dip of the solid curve of Fig. 5, which we tentatively interpret as damping deficiency. The scatter in Fig. 9 is remarkably small, and substantiates Gurtovenko and Kostik's (1982) claim of r.m.s. precision better than 0.1 dex.

The spread of the gf_w differences is larger than the spread of the gf_d differences. This may be due to the questionable use of microturbulence to take care of granulation (cf. Nordlund, 1981). We feel that the turbulence formalisms are a better simulator of the 5-min oscillation and internal gravity waves in higher layers, and we expect that the gf_d values will prove the better of the two sets when more laboratory data become available. However, the strongest high lines can have gf_d excesses when their gf_d values contain implicit corrections for NLTE excitation not fully masked by the HOLMUL model.

e) Choosing Between NLTE *and* LTE

Our NLTE reduction of the HOLMUL model to the HSRA shows that the two conflicting Fe I interpretations are fully reconciled by accepting the NLTE computations. The classical LTE interpretation is physically wrong, but it seems a numerically adequate shortcut in abundance studies of iron-like spectral species *provided that it is combined with a* NLTE-*masking model* like the HOLMUL photosphere: it then gives nearly correct answers. Also, one should *not* include the strongest downward transitions available for each upper-level excitation class, unless they are the ones actually used to set the upper part of the model, as multiplets 41 and 43 were by Holweger.

This recipe is *not* a reasonable shortcut for studies requiring the actual height of formation of lines, e.g. for magnetic or velocity diagnostics; such studies require comprehensive NLTE modeling such as Lites'. This course was indeed taken by Altrock et al. (1975) in deriving their list of formation heights for velocity lines[1].

f) Stellar Implications

The fortuitous success of the HOLMUL model in NLTE-masking is of interest to stellar abundance analyses. Empirical models for late-type stars determined from Fe I line-center intensities in Holweger's fashion are easy to derive, and may work equally well. An example is the empirical model for Aldebaran of Ramsey (1977), whose method (Ramsey and Johnson, 1975) is a reformulation of Holweger's for flux. Note that Ramsey biases his opacity scales per multiplet towards the initial model assumed; this will not be necessary when enough precise furnace oscillator strengths become available.

An interesting further shortcut is suggested by Fig. 1b, which shows the elaborate theoretical solar model of Bell et al. (1976, called BELLEA), in addition to the empirical models discussed above. This LTE radiative-equilibrium line-blanketed model is remarkably close to the HOLMUL model in the upper photosphere, and so will achieve good NLTE-masking equally fortuitously. Indeed, Gustafsson and Bell (1979) find that this model reproduces solar lines near $\lambda = 350$ nm quite well. If there is a reason for this close correspondence of empirical and theoretical LTE models in the upper photosphere, and if the same reason applies to other late-type stars with similar results, then theoretical LTE-RE models may actually be better stellar line profile predictors than their LTE basis warrants. However, the correspondence may very well be superficial; only detailed NLTE modeling, for every stellar case, can ascertain its significance (see Rutten and Cram, 1981, p. 489). We stress that this should first be done for the Sun.

Acknowledgements. We are indebted to Dr. C. Zwaan for many discussions and suggestions, and to Drs. A. A. van Ballegooijen, L.

1 Note that they used the opacity response function of Beckers and Milkey (1975), which is a special case of the general response function introduced by Mein (1971) (see also Caccin et al., 1977), and which is valid here because Fe I line source functions are generally in LTE. In our experiments above we have simply employed the intensity contribution function. The differences are not important here because the LTE-NLTE opacity corrections lead to similar shifts in both

E. Cram, H. Holweger, and B. W. Lites for comments on an intermediate manuscript. This work was begun while R. J. R. was guest of the Ukrainian Academy of Sciences at Kiev which he gratefully acknowledges, in particular the warm hospitality of Dr. E. A. Gurtovenko.

References

Altrock, R.C., November, L.J., Simon, G.W., Milkey, R.W., Worden, S.P.: 1975, *Solar Phys.* **43**, 33

Athay, R.G.: 1972, Radiation Transport in Spectral Lines, Reidel, Dordrecht

Athay, R.G., Lites, B.W.: 1972, *Astrophys. J.* **176**, 809

Auer, L.H., Heasley, J.N., Milkey, R.W.: 1972, *Kitt Peak Nat. Obs. Contrib.* No. 555

Beckers, J.M., Milkey, R.W.: 1975, *Solar Phys.* **43**, 289

Bell, R.A., Eriksson, K., Gustafsson, B., Nordlund, A.: 1976, *Astron. Astrophys. Suppl.* **23**, 37

Blackwell, D.E., Ibbetson, P.A., Petford, A.D., Shallis, M.J.: 1979, *Monthly Notices Roy. Astron. Soc.* **186**, 633

Blackwell, D.E., Petford, A.D., Shallis, M.J.: 1979, *Monthly Notices Roy. Astron. Soc.* **186**, 657

Blackwell, D.E., Shallis, M.J.: 1979, *Monthly Notices Roy. Astron. Soc.* **186**, 673

Blackwell, D.E., Shallis, M.J., Simmons, G.J.: 1980, *Astron. Astrophys.* **81**, 340

Brückner, K.A.: 1971, *Astrophys. J.* **169**, 621

Caccin, B., Gomez, M.T., Marmolino, C., Severino, G.: 1977, *Astron. Astrophys.* **54**, 227

Cram, L.E., Rutten, R.J., Lites, B.W.: 1980, *Astrophys. J.* **241**, 374

Crosswhite, H.M.: 1975, *J. Research N.B.S.* **79A**, 17

Delbouille, L., Roland, G., Neven, L.: 1973, Photometric Atlas of the Solar Spectrum from λ3000 to λ10,000, Institut d'Astrophysique, Liège

Deridder, G., van Rensbergen, W.: 1976, *Astron. Astrophys. Suppl.* **23**, 147

Dravins, D., Lindegren, L., Nordlund, A.: 1981, *Astron. Astrophys.* **96**, 345

Gehlsen, M., Holweger, H., Danzmann, K., Kock, M., Kühne, M.: 1978, *Astron. Astrophys.* **64**, 285

Gingerich, O., Noyes, R.W., Kalkofen, W., Cuny, Y.: 1971, *Solar Phys.* **18**, 347

Gurtovenko, E.A., Kostik, R.I.: 1980, Report ITF-79-138R of the Institute of Theoretical Physics, Ukrainian Academy of Sciences, Kiev (in Russian)

Gurtovenko, E.A., Kostik, R.I.: 1981, *Astron. Astrophys. Suppl.* **46**, 239

Gurtovenko, E.A., Kostik, R.I.: 1982, *Astron. Astrophys. Suppl.* **47**, 193

Gustafsson, B., Bell, R.A.: 1979, *Astron. Astrophys.* **74**, 313

Harvey, J.W.: 1973, *Solar Phys.* **28**, 9

Henze, W.: 1969, *Solar Phys.* **9**, 65

Holweger, H.: 1967, *Z. Astrophys.* **65**, 365

Holweger, H., Gehlsen, M., Ruland, F.: 1978, *Astron. Astrophys.* **70**, 537

Holweger, H., Müller, E.A.: 1974, *Solar Phys.* **39**, 19

Irwin, A.W.: 1979, *Monthly Notices Roy. Astron. Soc.* **188**, 707

Jefferies, J.T.: 1968, Spectral Line Formation, Blaisdell Publ. Co., Waltham (Mass.)

Lites, B.W.: 1972, NCAR Cooperative Thesis No. 28, Univ. of Colorado and High Altitude Observatory, NCAR, Boulder

Lites, B.W.: 1973, *Solar Phys.* **32**, 283

Lites, B.W., Brault, J.W.: 1972, *Solar Phys.* **30**, 283

Lites, B.W., White, O.R.: 1973, High Altitude Observatory Research Memorandum No. 185, Boulder

Mein, P.: 1971, *Solar Phys.* **20**, 7

Menzel, D.H., Cillié, G.G.: 1937, *Astrophys. J.* **85**, 88

Mihalas, D.: 1978, Stellar Atmospheres, 2nd ed., Freeman, San Francisco

Milkey, R.W.: 1976, in *Interpretation of Atmospheric Structure in the Presence of Inhomogeneities*, ed. C. J. Cannon, University of Sydney Printing Office

Moore, Ch.: 1959, A Multiplet Table of Astrophysical Interest, Nat. Bur. Stands. Techn. Note 36, Washington, Revised Edition

Moore, Ch.E., Merrill, P.W.: 1968, Partial Grotrian diagrams of Astrophysical Interest, *Natl. Bur. Stands. NSRDS-NBS* 23, Washington

Moore, Ch.E., Minnaert, M.G.J., Houtgast, J.: 1966, The Solar Spectrum 2935 Å–8770 Å, *Natl. Bur. Stands. Monograph* No. 61, Washington

Nordlund, A.: 1980, in *Stellar Turbulence*, D. F. Gray and J. L. Linsky (eds.) IAU *Coll.* **51**, Lecture Notes in Physics, Vol. 114, Springer, Berlin, Heidelberg, New York, p. 213

O'Neill, J.A., Smith, G.: 1980, *Astron. Astrophys.* **81**, 108

Pierce, A.K.: 1968, *Astrophys. J. Suppl.* **17**, 1

Ramsey, L.W.: 1977, *Astrophys. J.* **215**, 603

Ramsey, L.W., Johnson, H.R.: 1975, *Solar Phys.* **45**, 3

Rogerson, J.B.: 1969, *Astrophys. J.* **158**, 797

Ruland, F., Holweger, H., Griffin, R., Griffin, R., Biehl, D.: 1980, *Astron. Astrophys.* **92**, 70

Rutten, R.J.: 1976, Solar Eclipse Observations and Ba II Line Formation, thesis, Utrecht Astronomical Reprints No. 365

Rutten, R.J., Milkey, R.W.: 1979, *Astrophys. J.* **231**, 277

Rutten, R.J., Stencel, R.E.: 1980, *Astron. Astrophys. Suppl.* **39**, 415

Rutten, R.J., Cram, L.E.: 1981, in *The Sun as a Star*, ed. S. D. Jordan, CNRS-NASA Monograph Series on Nonthermal Phenomena in Stellar Atmospheres, NASA SP-450

Rutten, R.J., Zwaan, C.: 1983, *Astron. Astrophys.* (in press)

Sistla, G., Harvey, J.W.: 1970, *Solar Phys.* **12**, 66

Smith, M.A.: 1974, *Astrophys. J.* **190**, 481

Smith, M.A.: 1974, *Astrophys. J.* **192**, 623

Stenflo, J.O., Lindegren, L.: 1977, *Astron. Astrophys.* **59**, 367

Vernazza, J.E., Avrett, E.H., Loeser, R.: 1976, *Astrophys. J. Suppl.* **30**, 1

Vernazza, J.E., Avrett, E.H., Loeser, R.: 1981, *Astrophys. J. Suppl.* **45**, 350

Wijbenga, J.W., Zwaan, C.: 1972, *Solar Phys.* **23**, 265